DESY-02-187
hep-ex/0211033
20-11-2002

J/ψ Production via χ_c Decays in 920 GeV pA Interactions

The HERA-B Collaboration

I. Abt[28], A. Abyzov[26], M. Adams[11], H. Albrecht[13], V. Amaral[8], A. Amorim[8], S. J. Aplin[13], A. Arefiev[25], I. Ariño[2], M. Atiya[36], V. Aushev[18], Y. Bagaturia[13,43], R. Baghshetsyan[13,44], V. Balagura[25], M. Bargiotti[6], S. Barsuk[25], O. Barsukova[26], V. Bassetti[12], J. Bastos[8], C. Bauer[15], Th. S. Bauer[32,33], M. Beck[30], A. Belkov[26], Ar. Belkov[26], I. Belotelov[26], I. Belyaev[25], K. Berkhan[34], A. Bertin[6], B. Bobchenko[25], M. Böcker[31], A. Bogatyrev[25], G. Bohm[34], C. Borgmeier[5], M. Bräuer[15], D. Broemmelsiek[12], M. Bruinsma[32,33], M. Bruschi[6], P. Buchholz[31], M. Buchler[10], T. Buran[29], M. Capeáns[13], M. Capponi[6], J. Carvalho[8], J. Chamanina[27], B. X. Chen[4], R. Chistov[25], M. Chmeissani[2], A. Christensen[29], P. Conde[2], C. Cruse[11], M. Dam[9], K. M. Danielsen[29], M. Danilov[25], S. De Castro[6], H. Deckers[5], K. Dehmelt[13], H. Deppe[16], B. Dolgoshein[27], X. Dong[3], H. B. Dreis[16], M. Dressel[28], D. Dujmic[1], R. Eckmann[1], V. Egorytchev[13], K. Ehret[15,11], V. Eiges[25], F. Eisele[16], D. Emeliyanov[13], S. Erhan[22], S. Essenov[25], L. Fabbri[6], P. Faccioli[6], W. Fallot-Burghardt[15], M. Feuerstack-Raible [16], J. Flammer[13], H. Fleckenstein[13], B. Fominykh[25], S. Fourletov[27], T. Fuljahn[13], M. Funcke[11], D. Galli[6], A. Garcia[2], Ll. Garrido[2], D. Gascon[2], A. Gellrich[34,5,13], K. E. K. Gerndt[13], B. Giacobbe[6], J. Gläß[24], T. Glebe[15], D. Goloubkov[13,39], A. Golutvin[25], I. Golutvin[26], I. Gorbounov[31], A. Gorišek[19], O. Gouchtchine[25], D. C. Goulart[7], S. Gradl[16], W. Gradl[16], Yu. Guilitsky[25,13,41], T. Hamacher[13,1], J. D. Hansen[9], R. Harr[10], C. Hast[13], S. Hausmann[16], J. M. Hernández[13,34], M. Hildebrandt[16], A. Hölscher[16], K. Höpfner[13], W. Hofmann[15], M. Hohlmann[13], T. Hott[16], W. Hulsbergen[33], U. Husemann[31], O. Igonkina[25], M. Ispiryan[17], S. İşsever[11], H. Itterbeck[13], J. Ivarsson[23,34], T. Jagla[15], Y. Jia[3], C. Jiang[3], A. Kaoukher[27,30], H. Kapitza[11], S. Karabekyan[13,44], P. Karchin[10], N. Karpenko[26], Z. Ke[3], S. Keller[31], F. Khasanov[25], H. Kim[1], Yu. Kiryushin[26], I. Kisel[28], F. Klefenz[15], K. T. Knöpfle[15], V. Kochetkov[25], H. Kolanoski[5], S. Korpar[21,19], C. Krauss[16], P. Kreuzer[22,13], P. Križan[20,19], D. Krücker[5], T. Kvaratskheliia[25], A. Lange[31], A. Lanyov[26], K. Lau[17], G. Leffers[15], I. Legrand[34], B. Lewendel[13], Y. Q. Liu[4], T. Lohse[5], R. Loke[5], B. Lomonosov[13,38], J. Lüdemann[13], R. Männer[24], R. Mankel[5], U. Marconi[6], S. Masciocchi[28], I. Massa[6], I. Matchikhilian[25], G. Medin[5], M. Medinnis[13,22], M. Mevius[32], A. Michetti[13], Yu. Mikhailov[25,13,41], R. Miquel[2], R. Mizuk[25], A. Mohapatra[7], A. Moshkin[26], B. Moshous[28], R. Muresan[9], S. Nam[10], M. Negodaev[13,38], I. Négri[13], M. Nörenberg[13], S. Nowak[34], M. T. Núñez Pardo de Vera[13], T. Oest[14,13], A. Oliveira[8], M. Ouchrif[32,33], F. Ould-Saada[29], C. Padilla[13], P. Pakhlov[25], Yu.Pavlenko[18], D. Peralta[2], R. Pernack[30], T. Perschke[28], R. Pestotnik[19], B. AA. Petersen[9], M. Piccinini[6], M. A. Pleier[15], M. Poli[37], V. Popov[25], A. Pose[34], D. Pose[26,16], V. Pugatch[15,18], Y. Pylypchenko[29], J. Pyrlik[17], S. Ramachandran[17], F. Ratnikov[13,25], K. Reeves[1,15], D. Reßing[13], K. Riechmann[28], J. Rieling[15], M. Rietz[28], I. Riu[13], P. Robmann[35], J. Rosen[12], Ch. Rothe[13], W. Ruckstuhl[33,†], V. Rusinov[25], V. Rybnikov[13], D. Ryzhikov[13,40], F. Saadi-Lüdemann[13], D. Samtleben[14], F. Sánchez[13,15], M. Sang[28], V. Saveliev[27],

A. Sbrizzi[33], S. Schaller[28], P. Schlein[22], M. Schmelling[15], B. Schmidt[13,16], S. Schmidt[9], W. Schmidt-Parzefall[14], A. Schreiner[34], H. Schröder[13,30], H.D. Schultz[13], U. Schwanke[34], A. J. Schwartz[7], A. S. Schwarz[13], B. Schwenninger[11], B. Schwingenheuer[15], R. Schwitters[1], F. Sciacca[15], S. Semenov[25], N. Semprini-Cesari[6], E. Sexauer[15], L. Seybold[15], J. Shiu[10], S. Shuvalov[25,5], I. Siccama[13], D. Škrk[19], L. Sözüer[13], A. Soldatov[25,13,41], S. Solunin[26], A. Somov[5,13], S. Somov[13,39], V. Souvorov[34], M. Spahn[15], J. Spengler[15], R. Spighi[6], A. Spiridonov[34,25], S. Spratte[11], A. Stanovnik[20,19], M. Starič[19], R. StDenis[28,15], C. Stegmann[34,5], S. Steinbeck[14], O. Steinkamp[33], D. Stieler[31], U. Straumann[16], F. Sun[34], H. Sun[3], M. Symalla[11], S. Takach[10], N. Tesch[13], H. Thurn[13], I. Tikhomirov[25], M. Titov[25], U. Trunk[15], P. Truöl[35], I. Tsakov[13,42], U. Uwer[5,16], V. Vagnoni[6], C. van Eldik[11], R. van Staa[14], Yu. Vassiliev[18,11], M. Villa[6], A. Vitale[6], I. Vukotic[5], G. Wagner[13], W. Wagner[28], H. Wahlberg[32], A. H. Walenta[31], M. Walter[34], T. Walter[35], J. J. Wang[4], Y. M. Wang[4], R. Wanke[15], D. Wegener[11], U. Werthenbach[31], P. J. Weyers[5], H. Wolters[8], R. Wurth[13], A. Wurz[24], S. Xella-Hansen[9], J. Yang[4], Yu. Zaitsev[25], M. Zavertyaev[15,38], G. Zech[31], T. Zeuner[31], A. Zhelezov[25], Z. Zheng[3], Z. Zhu[3], R. Zimmermann[30], T. Živko[19], A. Zoccoli[6], J. Zweizig[13,22]

[1] *Department of Physics, University of Texas, Austin, TX 78712-1081, USA*[a]
[2] *Department ECM, Faculty of Physics, University of Barcelona, E-08028 Barcelona, Spain* [b]
[3] *Institute for High Energy Physics, Beijing 100039, P.R. China*
[4] *Institute of Engineering Physics, Tsinghua University, Beijing 100084, P.R. China*
[5] *Institut für Physik, Humboldt-Universität zu Berlin, D-10115 Berlin, Germany* [c]
[6] *Dipartimento di Fisica dell' Università di Bologna and INFN Sezione di Bologna, I-40126Bologna, Italy*
[7] *Department of Physics, University of Cincinnati, Cincinnati, Ohio 45221, USA*[a]
[8] *LIP Coimbra and Lisboa, P-3004-516 Coimbra, Portugal* [d]
[9] *Niels Bohr Institutet, DK 2100 Copenhagen, Denmark* [e]
[10] *Department of Physics and Astronomy, Wayne State University, Detroit, MI 48202, USA* [a]
[11] *Institut für Physik, Universität Dortmund, D-44227 Dortmund, Germany* [c]
[12] *Northwestern University, Evanston, Il 60208, USA*[a]
[13] *DESY, D-22603 Hamburg, Germany*
[14] *Institut für Experimentalphysik, Universität Hamburg, D-22761 Hamburg, Germany* [c]
[15] *Max-Planck-Institut für Kernphysik, D-69117 Heidelberg, Germany* [c]
[16] *Physikalisches Institut, Universität Heidelberg, D-69120 Heidelberg, Germany* [c]
[17] *Department of Physics, University of Houston, Houston, TX 77204, USA* [a,f]
[18] *Institute for Nuclear Research, Ukrainian Academy of Science, 03680 Kiev, Ukraine* [g]
[19] *J. Stefan Institute, 1001 Ljubljana, Slovenia*
[20] *University of Ljubljana, 1001 Ljubljana, Slovenia*
[21] *University of Maribor, 2000 Maribor, Slovenia*
[22] *University of California, Los Angeles, CA 90024, USA*[h]
[23] *Lund University, S-22362 Lund, Sweden*
[24] *Lehrstuhl für Informatik V, Universität Mannheim, D-68131 Mannheim, Germany*
[25] *Institute of Theoretical and Experimental Physics, 117259 Moscow, Russia* [i]
[26] *Joint Institute for Nuclear Research Dubna, 141980 Dubna, Moscow region, Russia*
[27] *Moscow Physical Engineering Institute, 115409 Moscow, Russia*
[28] *Max-Planck-Institut für Physik, Werner-Heisenberg-Institut, D-80805 München, Germany* [c]
[29] *Dept. of Physics, University of Oslo, N-0316 Oslo, Norway* [j]
[30] *Fachbereich Physik, Universität Rostock, D-18051 Rostock, Germany* [c]

[31] *Fachbereich Physik, Universität Siegen, D-057068 Siegen, Germany* [c]
[32] *Universiteit Utrecht/NIKHEF, 3584 CB Utrecht, The Netherlands* [k]
[33] *NIKHEF, 1009 DB Amsterdam, The Netherlands* [k]
[34] *DESY Zeuthen, D-15738 Zeuthen, Germany*
[35] *Physik-Institut, Universität Zürich, CH-8057 Zürich, Switzerland* [l]
[36] *Brookhaven National Laboratory, Upton, NY 11973, USA*
[37] *visitor from Dipartimento di Energetica dell' Università di Firenze and INFN Sezione di Bologna, Italy*
[38] *visitor from P.N. Lebedev Physical Institute, 117924 Moscow B-333, Russia*
[39] *visitor from Moscow Physical Engineering Institute, 115409 Moscow, Russia*
[40] *visitor from Institute of Nuclear Power Engineering, 249030, Obninsk, Russia*
[41] *visitor from Institute for High Energy Physics, Protvino, Russia*
[42] *visitor from Institute for Nuclear Research, INRNE-BAS, Sofia, Bulgaria*
[43] *visitor from High Energy Physics Institute, 380086 Tbilisi, Georgia*
[44] *visitor from Yerevan Physics Institute, Yerevan, Armenia*

[†] *deceased*

[a] *supported by the U.S. Department of Energy (DOE)*
[b] *supported by the CICYT contract AEN99-0483*
[c] *supported by the Bundesministerium für Bildung und Forschung, FRG, under contract numbers 05-7BU35I, 05-7DO55P, 05 HB1HRA, 05 HB1KHA, 05 HB1PEA, 05 HB1PSA, 05 HB1VHA, 05 HB9HRA, 05 7HD15I, 05 7HH25I, 05 7MP25I, 05 7SI75I*
[d] *supported by the Portuguese Fundação para a Ciência e Tecnologia*
[e] *supported by the Danish Natural Science Research Council*
[f] *supported by the Texas Advanced Research Program*
[g] *supported by the National Academy of Science and the Ministry of Education and Science of Ukraine*
[h] *supported by the U.S. National Science Foundation Grant PHY-9986703*
[i] *supported by the Russion Fundamental Research Foundation under grant RFFI-00-15-96584 and the BMBF via the Max Planck Research Award*
[j] *supported by the Norwegian Research Council*
[k] *supported by the Foundation for Fundamental Research on Matter (FOM), 3502 GA Utrecht, The Netherlands*
[l] *supported by the Swiss National Science Foundation*

Abstract

Using data collected by the HERA-B experiment, we have measured the fraction of J/ψ's produced via radiative χ_c decays in interactions of 920 GeV protons with carbon and titanium targets. We obtained $R_{\chi_c} = 0.32 \pm 0.06_{stat} \pm 0.04_{sys}$ for the fraction of J/ψ from χ_c decays averaged over proton-carbon and proton-titanium collisions. This result is in agreement with previous measurements and is compared with theoretical predictions.

PACS: [13.85.Ni], [13.85.Qk], [24.85.+p], [24.85.Eqp]

1 Introduction

The mechanism by which quarkonium states are produced in hadronic collisions is not understood and is a subject of current interest. At present, several models exist. The Colour Singlet Model (CSM) [1] requires that the $q\bar{q}$ pair be produced in a colour singlet state with the quantum numbers of the final meson. The Non-Relativistic QCD factorisation approach (NRQCD) [2, 3] assumes that a colour singlet or colour octet quark pair evolves towards the final bound state via exchange of soft gluons. The nonperturbative part of the process is described by long distance matrix elements which are extracted from data. Finally, the Colour Evaporation Model (CEM) [4, 5] assumes the exchange of many soft gluons during the formation process such that the final meson carries no information about the production process of the $q\bar{q}$ pair.

Charmonium production is an attractive test case as the quarks are heavy enough for perturbative calculations of the $q\bar{q}$ production process, yet the cross sections are large enough to be measured with good statistics. The dependence of the ratio of production cross sections for different states, e.g. the ratio of χ_c[1] and J/ψ production cross sections $\sigma(\chi_c)/\sigma(J/\psi)$, on $\sqrt{s}$ or the projectile allows one to distinguish among different models. From the experimental point of view, the specific decay $\chi_c \to J/\psi\,\gamma$ is advantageous since the decay signature $J/\psi \to \ell^+\ell^-$ ($\ell = \mu, e$) can be used as trigger requirement. Furthermore, several systematic errors cancel in the ratio, and the only significant difference in the detection of the χ_c and the J/ψ is the photon reconstruction. Due to the small branching ratio of $\chi_{c0} \to J/\psi\,\gamma$, $(6.6 \pm 1.8) \cdot 10^{-3}$ [6], the χ_{c0} contribution to the reconstructed χ_c signal can be neglected. The χ_{c1} and χ_{c2} states, with radiative branching ratios of 0.273 ± 0.016 and 0.135 ± 0.011 [6], respectively, are separated by 46 MeV/c^2. In most experiments the energy resolution is insufficient to resolve these two states, so that one usually quotes the ratio

$$R_{\chi_c} = \frac{\sum_{i=1}^{2} \sigma(\chi_{ci}) Br(\chi_{ci} \to J/\psi\,\gamma)}{\sigma(J/\psi)}. \tag{1}$$

Here, $\sigma(J/\psi)$ is the sum of production cross sections for direct J/ψ's and J/ψ's produced in decays of χ_c and ψ'. In the same way, $\sigma(\chi_{ci})$ includes direct χ_c production and the feed-down from the ψ'. Contributions from η_c', h_c and heavier charmonia are neglected.

While this "inclusive" R_{χ_c} ratio is usually quoted in the literature, one can define the ratio for direct χ_c production over direct J/ψ production

$$R_{\chi_c}^{dir} = \frac{\sum_{i=1}^{2} \sigma(\chi_{ci})_{dir} Br(\chi_{ci} \to J/\psi\gamma)}{\sigma(J/\psi)_{dir}}. \tag{2}$$

$R_{\chi_c}^{dir}$ can be derived from R_{χ_c} and the known ratio of ψ' to J/ψ production cross sections [7] and known branching ratios [6].

The experimental situation is unclear, and the uncertainties are large particularly for proton induced reactions where the few existing measurements of R_{χ_c} [8] differ strongly. Measurements made with pion beams [9] have higher precision and may indicate that R_{χ_c} increases with $\sqrt{s}$. For photon and electron-induced reactions, only upper limits for R_{χ_c} have been reported [10].

We report here a new determination of R_{χ_c} in interactions of 920 GeV protons with carbon and titanium nuclei. The χ_c is observed in the decay $\chi_c \to J/\psi\gamma \to \ell^+\ell^-\gamma$ ($\ell = \mu, e$) using the value ΔM, which is the difference between the invariant mass of the $(\ell^+\ell^-\gamma)$ system and the invariant mass of the

[1] In the following, the notation "χ_c" indicates the sum of the three states χ_{c0}, χ_{c1} and χ_{c2}.

lepton pair $\ell^+\ell^-$:

$$\Delta M = M(\ell^+\ell^-\gamma) - M(\ell^+\ell^-). \tag{3}$$

Here, the uncertainty in the determination of the J/ψ mass essentially cancels. An excess of events with respect to the combinatorial background determines the number of χ_c candidates N_{χ_c}, from which the "inclusive" value, R_{χ_c}, can be calculated as follows:

$$R_{\chi_c} = \frac{N_{\chi_c}}{N_{J/\psi} \cdot \varepsilon_\gamma} \cdot \rho_\varepsilon, \tag{4}$$

where $N_{J/\psi}$ is the total number of reconstructed $J/\psi \to \ell^+\ell^-$ decays used for the χ_c search. The factor ε_γ is the photon detection efficiency. The value ρ_ε represents the ratio of trigger and reconstruction efficiencies for J/ψ's from χ_c decays and for all J/ψ's:

$$\rho_\varepsilon = \frac{\varepsilon_{trig}^{J/\psi}}{\varepsilon_{trig}^{\chi_c}} \frac{\varepsilon_{reco}^{J/\psi}}{\varepsilon_{reco}^{\chi_c}}. \tag{5}$$

Since the kinematics, triggering and reconstruction of direct J/ψ's and J/ψ's from χ_c decays are very similar, ρ_ε is close to unity.

2 Detector, Trigger and Data Sample

HERA-B is a fixed target experiment operating at the HERA storage ring at DESY. Charmonium and other heavy flavour states are produced in inelastic collisions by inserting wire targets into the halo of the 920 GeV proton beam circulating in HERA. The pN ($N = p, n$) c.m.s. energy is $\sqrt{s} = 41.6$ GeV.

The detector is a magnetic spectrometer emphasising vertexing, tracking and particle identification, with a dedicated J/ψ-trigger. The components of the HERA-B detector used for this analysis include a silicon strip vertex detector (VDS), honeycomb drift chambers (OTR), a large acceptance 2.13 T·m magnet, a finely segmented "shashlik" electromagnetic calorimeter (ECAL), and a muon system (MUON) consisting of wire chambers interleaved with iron shielding which detects muons with momenta larger than 5 GeV/c. The ECAL is divided into three radial parts with decreasing granularities, of which two, the "inner" and "middle" sections, are used for the measurement described here. The performance of the calorimeter is described in Ref. [11]. The HERA-B detector allows an efficient reconstruction of particles with momenta larger than 1 GeV/c, including γ's and π^0's, within the acceptance. A detailed description of the apparatus is given in Ref. [12].

The HERA-B target station houses 8 target wires which can be moved independently into the beam halo. Their positions are steered such that the proton interaction rates are equalised for the targets in use. The data presented here were obtained using a carbon wire and a titanium wire separated by 3.3 cm along the beam direction. The resolution of the reconstructed dilepton vertices of 0.6 mm along the beam direction [13] allows a clear association of the interaction to a specific target wire. The analysis presented is based on data collected during a short commissioning run in summer 2000. About half of the data was taken with a single carbon wire; the second half was taken with carbon and titanium wires together. The proton-nucleus interaction rate was approximately 5 MHz.

The trigger selects $\mu^+\mu^-$ and e^+e^- pairs, the latter with an invariant mass larger than 2 GeV/c^2. For a muon candidate the trigger requires at least 3 MUON hits in coincidence with 9 OTR hits consistent with a particle track with a transverse momentum between 0.7 GeV/c and 2.5 GeV/c. The electron

trigger requires that the transverse energy deposited in the calorimeter[2] by the electron candidates be greater than 1.0 GeV and that at least 9 OTR hits confirm the track hypothesis. Both muon and electron candidates have to be confirmed by a track segment in the vertex detector with at least 6 hits. For the data described here, the trigger acceptance for J/ψ's was limited to the x_F range $-0.25 < x_F < 0.15$, x_F being the Feynman's x variable. For more details concerning the trigger and the data sample of the year 2000 run, see Ref. [14].

The data is divided into four separate samples: $\mu^+\mu^-$ or e^+e^- final states, each originating from either carbon or titanium target wires (μ-C, e-C, μ-Ti and e-Ti).

3 Monte Carlo Simulation

At present, NRQCD is the favoured approach to describe charmonium formation. It is therefore used to generate our signal Monte Carlo sample. To estimate the model dependence systematics we use the CSM. Since the CEM does not make any conclusive predictions for the differential charmonium production cross sections, we have not used it in the simulations.

The Monte Carlo simulation (MC) of events is done in three steps. First, a J/ψ or χ_c is generated using PYTHIA 5.7 [15]. In the simulations, the CTEQ2L parton density function [15] and the c quark mass $m_c = 1.48$ GeV/c^2 are used. The sum of the transverse momenta of the reaction products must exceed 0.5 GeV/c. Any polarisation is neglected. For NRQCD, the differential cross sections and long distance matrix elements are taken from Ref. [3]. For CSM, the differential cross sections are taken from Ref [1]. During the second step, the energy remaining after the charmonium generation is used to simulate the rest of the pA interaction using FRITIOF 7.02 [16]. Finally, the J/ψ event is combined with n other inelastic interactions to simulate several interactions per event, as observed in the data. The number n is distributed according to Poisson statistics with a mean value of 0.5 determined from the mean experimental interaction rate.

The detector response is simulated using GEANT 3.21 [17] and includes the measured hit resolution, the mapping of inefficient channels, and electronic noise. The simulated events are processed by the same trigger and reconstruction codes as the data. The simulation has been checked to ensure that it accurately describes the detector, both in terms of geometric acceptance and material composition (see sect. 4.6). From the MC we expect a mass resolution for the χ_c signal of 45 MeV/c^2, which is insufficient to separate the χ_{c1} and χ_{c2} states.

MC studies show that the trigger and reconstruction efficiencies for $J/\psi \to \ell^+\ell^-$ are indeed similar for both direct J/ψ's and for those originating from $\chi_c \to J/\psi\,\gamma$ decays. We obtain $\rho_\varepsilon = 0.95 \pm 0.02$ for the NRQCD and $\rho_\varepsilon = 0.97 \pm 0.01$ for the CSM. For the measurement we use the NRQCD value $\rho_\varepsilon = 0.95$ and consider the difference between the two values as a measure of the systematic uncertainty of ρ_ε (see sect. 4.6).

The Monte Carlo sample used in the analysis is about six times larger than the data sample.

[2]The transverse energy is defined as cluster energy multiplied by the transverse distance to the beam axis and divided by the cluster-target distance.

4 Data Analysis

4.1 Method and Selection Criteria

The analysis consists of the reconstruction of the J/ψ events, the search for the photon candidates in the ECAL, and the determination of the invariant mass of the J/ψ and photon candidates within the event. The selection criteria for the χ_c are tuned to maximise the quantity $N_{J/\psi} \cdot \varepsilon_\gamma / \sqrt{N}$. Here, $N_{J/\psi}$ is the number of J/ψ candidates above background found in the data, and ε_γ is the photon reconstruction efficiency determined from MC simulations. N is the number of all events, including background, found in the measured ΔM distribution within a window of two standard deviations (determined from MC) around the expected χ_c position. The procedure is applied for all cuts described below.

4.2 J/ψ Selection

In the offline analysis, a track is selected as a muon candidate if its transverse momentum is greater than 0.7 GeV/c and the muon likelihood, derived from the ratio of the expected and found MUON hits, is greater than 0.001. The latter removes hit combinatorics which satisfy the trigger while keeping nearly all good muons.

A track is identified as an electron candidate if *(a)* the transverse energy (E_T) is greater than 1 GeV; and *(b)* it has $|E/p - 1| < 0.3$, where E is the energy deposited in the calorimeter and p is the track momentum. The cut on E/p corresponds to about 3.3 standard deviations of the electron E/p distribution. To further reject the background from hadrons, a search for associated bremsstrahlung photons emitted in the region upstream of, or inside, the magnet is performed for each electron candidate. Thus, an isolated electromagnetic cluster is required in the area where the bremsstrahlung would hit the ECAL. The energy of the bremsstrahlung cluster is added to the energy of the electron candidate. The requirement of an associated bremsstrahlung photon candidate for each of the two electron candidates of the $J/\psi \to e^+e^-$ decay has an efficiency ε_{brem} of about 20% (about 45% per electron) and suppresses the background by a factor of 45. These values are obtained by comparing the J/ψ and background rates under this requirement with those for the case that at least one of the two electrons is associated with a bremsstrahlung cluster, and they are also confirmed by MC studies (see alse sect. 4.6).

The assignment of the J/ψ candidates to a target wire is based on the position of the reconstructed dilepton vertex. The χ^2 probability of this vertex is required to be larger than 0.005 to eliminate spurious events.

The invariant mass is calculated for each opposite-charge lepton pair. The resulting mass distributions are shown in Fig. 1 for each of the four samples. The signal observed for $J/\psi \to \mu^+\mu^-$ events is Gaussian while the $J/\psi \to e^+e^-$ signal has an asymmetric bremsstrahlung tail. In both cases the background underneath the signal comes mainly from misidentified hadrons and conversions. The background shape is either described by an exponential distribution ($\mu^+\mu^-$) or by an exponential multiplied by a second order polynomial distribution (e^+e^-). The shape is confirmed by the invariant mass distribution of the same sign candidates in the muon case, and by fitting the distribution that results from using all trigger candidates (mostly hadrons) in the electron case. Only J/ψ candidates within a two standard deviation ($2\ \sigma$) window around the J/ψ mass are considered for the analysis. In the electron case, σ is taken from the high mass part of the signal which is Gaussian. The numbers of J/ψ candidates obtained from the fit and corrected for the mass window are shown in Table 1 for the four samples.

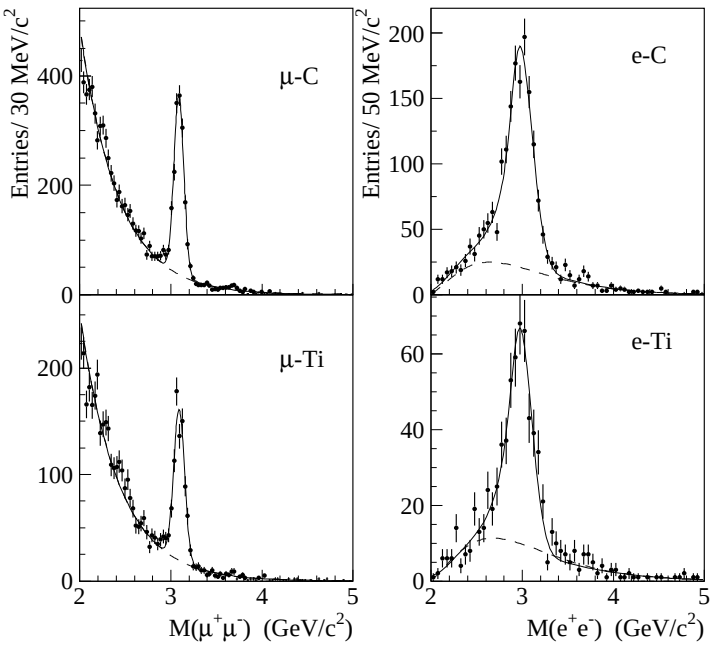

Figure 1: Dilepton invariant mass spectrum for each of the four samples (μ-C, μ-Ti, e-C, e-Ti). The dashed lines show the estimated background under the J/ψ signal. See text for the details on the fits (solid lines). The selection criteria are described in sects. 4.2 and 4.3.

4.3 Particle Multiplicities

Detector occupancies have a considerable impact on the χ_c reconstruction: large calorimeter occupancies lead to more combinatorial background. However, detector occupancies are correlated with particle multiplicities and thus depend on the underlying physics of the event. Since the cross section for J/ψ and χ_c production are of the same order of magnitude, and the kinematic dependence of direct J/ψ and those from χ_c decays are similar, we assume both types of events to have similar particle multiplicities excluding the decay products of charmonium. The charged particle multiplicity is proportional to the number of tracks reconstructed in the VDS. We eliminate especially "busy" events which tend to contribute more to the background than to the signal. Based on the multiplicity distributions we require that there are not more than 30 (34) VDS tracks in events with a J/ψ candidate originating from the carbon (titanium) target. We also require less than 19 clusters in the ECAL. The upper limit on the number of tracks reduces the background under the J/ψ signal while the cut on the number of clusters limits the combinatorial background under the χ_c. The numbers of J/ψ's passing the multiplicity cuts are given in Table 1.

4.4 Photon Selection

Each cluster in the ECAL with $E_T > 0.1$ GeV that is not associated with the leptons from the J/ψ, is considered as a photon candidate. The area of the ECAL closest to the proton beam pipe $x^2/4 + y^2 < 484$ cm^2 (or equivalently : $\theta_x^2/4 + \theta_y^2 < 265$ mrad^2) is excluded, as the occupancy in this region is high (up to 30%). Hadronic background is reduced by requiring that the ratio of the central cell energy to

the total cluster energy (E_{centr}/E) be greater than 0.6. In order to suppress background due to soft secondary particles and noise clusters, an energy cut $E > 3.0$ GeV is applied. A charged track veto is not applied, due to a 44% probability of the photon to convert in the detector material downstream of the magnet. The material of the detector in front of the ECAL causes photon conversion, and thus losses of photons from χ_c's. We determine these losses using MC simulations.

Since the relative momenta of the J/ψ and the photon from the χ_c decay are correlated, a cut in the acceptance of the J/ψ affects the acceptance for the photon as well. The electron sample, with a slightly larger acceptance close to the beam as compared to the muon sample, also contains more energetic photons than the muon sample. The different samples have different kinematics and acceptances, leading to different photon detection efficiencies which are determined for each sample separately using MC simulations (see Table 1). The uncertainty in the photon detection efficiency arises mainly from the finite MC statistics; however, this uncertainty is insignificant compared to the statistical error on N_{χ_c}.

4.5 χ_c Reconstruction

The ΔM distributions for all combinations of J/ψ and photon candidates for the carbon samples are shown in Fig. 2. The distributions show a signal corresponding to the sum of the two charmonium states χ_{c1} and χ_{c2}.

Possible sources of background are random combinations of J/ψ and photon candidates, decays of heavier mesons into $J/\psi X$, and the radiative decay $J/\psi \to e^+e^-\gamma$. The fraction of J/ψ's originating from ψ' decays is about 8% [8]. The fraction of photons arising from $\psi' \to J/\psi\,\pi^0\pi^0$ decays which pass the energy cut $E > 3.0$ GeV is negligible, as is the fraction of pions misidentified as photons from $\psi' \to J/\psi\,\pi^-\pi^+$ decays. The fraction of J/ψ's resulting from decays of B-mesons, Υ, χ_b, η_c', and χ_{c0} is negligible as well. The photon from the radiative decay $J/\psi \to e^+e^-\gamma$, mostly oriented along the direction of one of the leptons, is indistinguishable from bremsstrahlung and, as such, is taken into account. In the muon sample, bremsstrahlung clusters are neither expected nor found above background. The fraction of such radiative decays is considered to be negligible. Thus the background consists mainly of random combinations of J/ψ and photon candidates.

The shape of the dominantly combinatorial background in the ΔM distribution is obtained by combining J/ψ candidates with photon candidates from different events with similar multiplicity and applying the standard selection cuts. These "mixed events" reproduce the shape of the ΔM distribution everywhere except in the χ_c signal region (see solid line in Fig. 2, left panel). Similar results are obtained when events in the sidebands of the J/ψ mass region are combined with photon candidates. Since the experimental resolution is of the same order as the mass difference between χ_{c1} and χ_{c2} states and the statistics is limited, we use a single Gaussian to describe the signal. In the fit, the position and normalisation of the Gaussian, as well as the normalisation of the background, are left free. The width of the Gaussian is fixed to the value predicted by MC based on the NRQCD approach (45 MeV/c^2), where the production cross section ratio of χ_{c1} and χ_{c2} is approximately 0.65. The position of the Gaussian agrees well with the value expected from MC. The background normalisation is also treated as a free parameter when we fit the number of $\chi_c \to J/\psi\,\gamma$ decays. The background subtracted distributions are shown in the right panel of Fig. 2. The significance of the signals seen in the μ-C and e-C samples is about three standard deviations. The obtained number of χ_c events as well as the number of J/ψ events and the photon detection efficiency are summarised in Table 1.

Taking into account the high background level and the ratio of N_{χ_c} to $N_{J/\psi}$ observed in the carbon samples, we do not expect to see a significant χ_c signal in the smaller titanium samples. The results obtained for the titanium sample with the same procedure are shown in Fig. 3. The starting value for

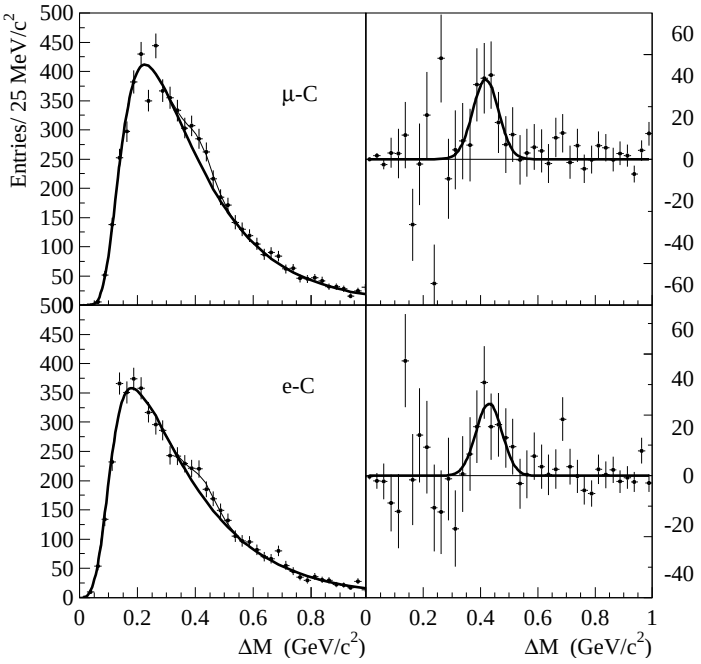

Figure 2: The $\Delta M = M(\ell^+\ell^-\gamma) - M(\ell^+\ell^-)$ distribution for samples μ-C and e-C. In the left-most plots, the points represent data and the solid lines represent the combinatorial background estimated by event mixing. The right-most plots show the signal after background subtraction. See text and Table 1 for the details on the fit.

the peak position has been taken from the fit of the carbon data. Although the signals are marginal, the R_{χ_c} values obtained from them are compatible with estimates from the carbon samples (see Table 1).

As a cross check, all four samples are combined together as shown in Fig. 4. The value of $N_{\chi_c} = 380 \pm 74$ obtained from this distribution agrees within the errors with the sum of the N_{χ_c} values obtained from the individual samples.

4.6 Study of the Systematic Uncertainties

The systematic uncertainty in the yield of $J/\psi \to e^+e^-$ candidates due to the background description is estimated to be 5%, whereas the uncertainty is negligible in the muon case.

The model dependence of the relative efficiency ρ_ε for all J/ψ's and J/ψ's from χ_c has been studied. A 2% difference of ρ_ε is found for the two models (NRQCD and CSM) for each of the J/ψ leptonic decay modes. For the same models a difference of the photon detection efficiency ε_γ integrated over all χ_c states is found to be 4%. In both cases the observed difference is treated as an estimate of the corresponding systematic uncertainty. The overall systematic error accounting for the model dependence of the selection efficiency is 5%.

To confirm the MC description of the detector material composition and acceptance which affects the photon detection efficiency, we compare the bremsstrahlung tag probability $\sqrt{\varepsilon_{brem}}$ determined from the data and MC. The values obtained, 0.44 ± 0.02 and 0.43 ± 0.01 for the data and MC, respectively, are compatible within one standard deviation. The systematic uncertainty due to photon losses is conservatively taken to be 2%.

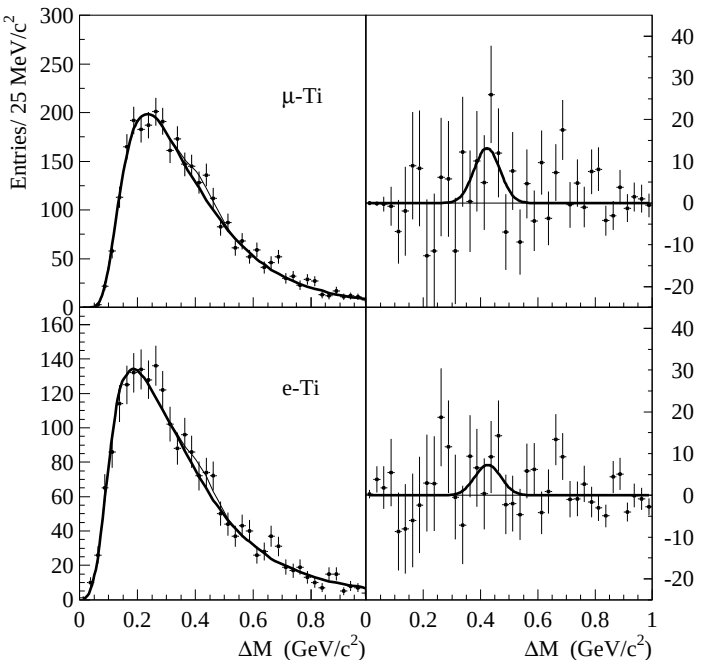

Figure 3: Same as in Fig. 2 for the μ-Ti and e-Ti samples.

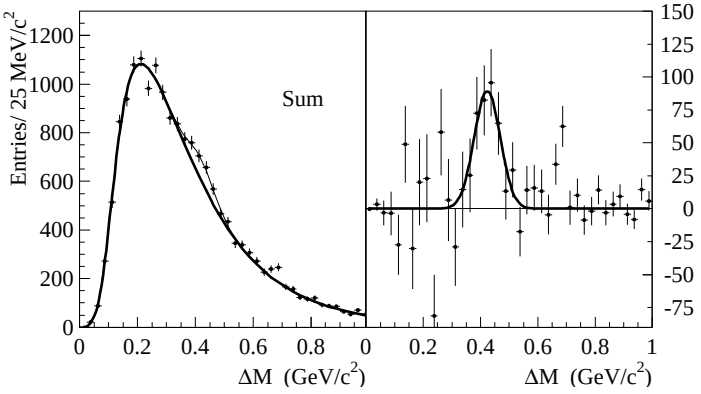

Figure 4: Same as in Fig. 2 for all data combined.

Table 1: The number of selected J/ψ events ($N_{J/\psi}^{selected}$), the number of J/ψ's passing the multiplicity cut ($N_{J/\psi}$), the number of χ_c's observed (N_{χ_c}), χ^2 per degree of freedom for the ΔM fit, photon detection efficiency (ε_γ), and the result for R_{χ_c}, for each of the four event samples. The quoted error on R_{χ_c} is statistical, excluding the systematic uncertainty in ε_γ.

	μ-C	e-C	μ-Ti	e-Ti
$N_{J/\psi}^{selected}$	1760 ± 48	1380 ± 69	765 ± 31	512 ± 41
$N_{J/\psi}$	1510 ± 44	1180 ± 59	643 ± 29	382 ± 32
N_{χ_c}	159 ± 47	121 ± 38	59 ± 33	31 ± 27
$\chi^2/n.d.f$	28/35	34/35	27/35	48/35
ε_γ (%)	27.3 ± 1.1	32.8 ± 1.5	24.4 ± 1.8	32.7 ± 2.6
R_{χ_c}	0.37 ± 0.11	0.30 ± 0.09	0.36 ± 0.20	0.23 ± 0.21

The effect of systematic uncertainties of the ECAL calibration is studied by using MC simulations. The level of possible uncertainties is determined from the data using the π^0 signal. The uncertainty of the π^0 calibration is used then in the MC simulations to determine its effect on the detection of the χ_c. The systematic uncertainty on R_{χ_c} due to this effect is estimated to be 1%.

Correlated electronic noise in the calorimeter can shift and widen the ΔM distribution of the χ_c signal. A cluster reconstruction procedure based on the known correlation between channels is developed to compensate for this effect. The numbers of events observed with and without this algorithm in the data agree with each other within the statistical errors. MC studies show that the corresponding relative systematic uncertainty is 3%.

The width of the χ_c signal in the ΔM distribution depends on the ratio of χ_{c1} and χ_{c2} and on the detector resolution, mainly that of the ECAL. When the width is left free to vary in the carbon data fit, the resulting width agrees within one standard deviation with the nominal one. A systematic error on R_{χ_c} of 6% is assigned based on an MC study of the signal resolution dependence on the χ_{c1} to χ_{c2} ratio and the ECAL resolution.

The stability of our results with respect to variations in the selection criteria is studied separately for the different samples. The ratio R_{χ_c} is measured as a function of the cuts on VDS track multiplicity, ECAL cluster multiplicity, photon energy E, and ratio E_{centr}/E. The variation of the cut on the photon energy E results in a variation of R_{χ_c} of 6%, which is taken as an estimate for the systematic uncertainty. The dependence on other cuts is negligible.

The systematic uncertainty on ε_γ due to the finite MC statistics is 3% as estimated from the weighted average of the values in Table 1.

The polarisation of the χ_c affects the reconstruction efficiency of χ_c, however with the present statistics we are not able to determine it. Thus, like the previous experiments, we have assumed no polarisation and have neglected the uncertainty related to it.

Assuming that all individual systematic errors are uncorrelated, an estimate of the total systematic uncertainty on R_{χ_c} is 11% (see Table 2).

Table 2: Contributions to the relative systematic uncertainty. For the calculation of the total uncertainty the correlation in the systematic errors of the different samples is taken into account.

	Uncertainty
J/ψ background shape (e-C, e-Ti only)	5%
Model dependence	5%
Photon losses	2%
ECAL calibration	1%
Correlated noise in ECAL	3%
ΔM resolution	6%
Dependence on cuts	6%
Finite MC statistics (ε_γ)	3%
Total	11%

5 Results

The values of R_{χ_c} obtained for all four samples are listed in Table 1. The results for the two carbon samples agree with each other within the statistical errors. The results obtained from the titanium data are consistent with those obtained from the carbon data.

Although nuclear dependence effects might be present in R_{χ_c} at the few percent level for the targets used here [19], they are beyond the statistical accuracy of the present measurement. We therefore average the results for the four samples obtaining:

$$\langle R_{\chi_c} \rangle \;=\; 0.32 \pm 0.06_{stat} \pm 0.04_{sys}. \tag{6}$$

The first uncertainty listed is statistical only, whereas the second uncertainty is systematic.

In order to extract the ratio $R_{\chi_c}^{dir}$ of the "direct" χ_c and J/ψ production, we use

$$R_{\chi_c}^{dir} = \frac{1 - R_\psi B_1}{1 - R_{\chi_c} - R_\psi B_1 + R_\psi B_2} - 1, \tag{7}$$

where $R_\psi = \sigma(\psi')/\sigma(J/\psi) = 0.094 \pm 0.035$ is taken from Ref. [7] and corrected for the branching ratios [6]. B_1 is the branching ratio $Br(\psi' \to J/\psi X)$ and B_2 is the sum of branching ratios $\sum_{i=1}^{2} Br(\psi' \to \chi_{ci}\gamma) Br(\chi_{ci} \to J/\psi\gamma)$ [6]. We obtain $R_{\chi_c}^{dir} = 0.50 \pm 0.15_{stat} \pm 0.08_{sys}$.

Our result for R_{χ_c} (eq. (6)) is compatible with most of the previous data ([8, 9] and [18]), as shown in Table 3 and Fig. 5. Due to the relatively large uncertainties, especially for the data on proton induced reactions, a flat energy dependence, as predicted by CEM [5], cannot be ruled out. Similarly, the slope of the energy dependence as predicted by the Monte Carlo based on NRQCD (see sect. 3) is also compatible with the data. However, the predictions of NRQCD seem to fall below the data, which might indicate that the NRQCD long distance matrix elements for χ_c production [3] used for the calculations are underestimated. On the other hand, CSM predicts values for R_{χ_c} which are larger than most of the data. More precise measurements, especially of proton induced reactions are needed to conclusively discriminate among these models.

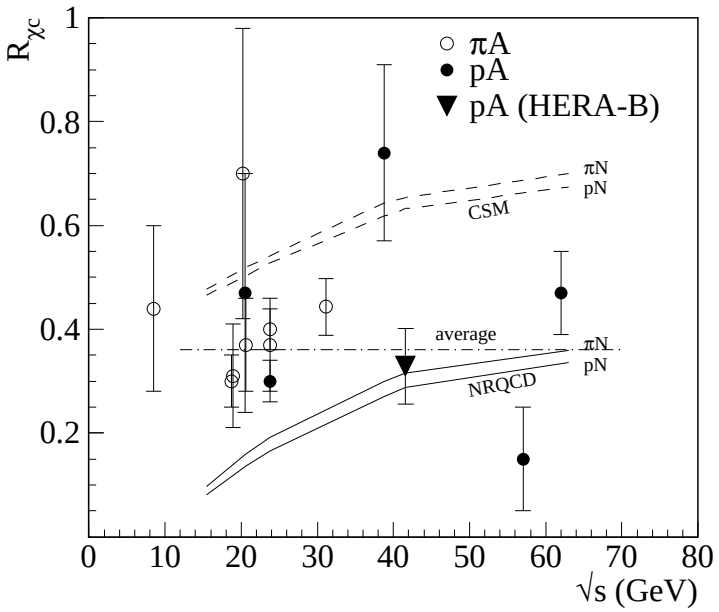

Figure 5: Comparison of our measurement of R_{χ_c} (closed triangle) with those of other pp, pA [8] (closed circles) and πp, πA [9] (open circles) experiments. The CDF result [18] is not shown, since its kinematic acceptance differs strongly from the other experiments. The value quoted for exp. E771 has been calculated from the published cross sections [8] and branching ratios [6]. The error bars include statistical and systematic uncertainties. Also shown are predictions for pN and πN interactions obtained from Monte Carlo based on the NRQCD [3] (solid), CSM [1] (dashed) (see sect. 3). The CEM [4, 5] predicts a constant value. The dot-dashed line is the average of all measurements.

Table 3: Previous πA [9], pA [8], $p\bar{p}$ [18] and HERA-B measurements of the R_{χ_c} value. The value quoted for exp. E771 has been calculated from the published cross sections [8] and branching ratios [6].

Exp.	coll.	$\sqrt{s}$ (GeV)	R_{χ_c}
IHEP140	$\pi^- p$	8.5	0.44 ± 0.16
WA11	π^-Be	18.7	0.30 ± 0.05
E610	π^-Be	18.9	0.31 ± 0.10
E673	π^-H$_2$, π^-Be	20.2	0.70 ± 0.28
E369	π^-Be	20.6	0.37 ± 0.09
E705	π^-Li	23.8	0.37 ± 0.03
E705	π^+Li	23.8	0.40 ± 0.04
E672/706	π^-Be	31.1	$0.443 \pm 0.041 \pm 0.035$
E610	pBe	19.4, 21.7	0.47 ± 0.23
E705	pLi	23.8	0.30 ± 0.04
E771	pSi	38.8	0.74 ± 0.17
R702	pp	52, 63	$0.15^{+0.10}_{-0.15}$
ISR	pp	62	0.47 ± 0.08
CDF	$p\bar{p}$	1800	$0.297 \pm 0.017 \pm 0.057$
HERA-B	pC, pTi	41.6	$0.32 \pm 0.06 \pm 0.04$

6 Conclusions

A measurement of the ratio of J/ψ produced via radiative χ_c decays to all produced J/ψ allows one to quantitatively test different models of quarkonium production. We present a new result from the HERA-B experiment for the fraction of J/ψ's originating from radiative decays of χ_{c1} and χ_{c2} states produced in pC and pTi interactions. The fraction of J/ψ's in the range of $-0.25 < x_F < 0.15$ originating from radiative χ_c decays is determined to be $R_{\chi_c} = 0.32 \pm 0.06_{stat} \pm 0.04_{sys}$, and consequently, the ratio of the cross section of directly produced χ_c's decaying into J/ψ to the cross section of directly produced J/ψ's is $R^{dir}_{\chi_c} = 0.50 \pm 0.15_{stat} \pm 0.08_{sys}$ in the above x_F range. The result has been obtained with C and Ti targets and detecting the J/ψ decay modes into electrons and muons. Our result for R_{χ_c} agrees with most previous proton and pion beam measurements, neglecting any possible energy dependence. It agrees also with the predictions of the Non-Relativistic QCD factorisation approach (NRQCD), whereas it falls significantly below the predictions of the Color Singlet Model (CSM).

Acknowledgements

We express our gratitude to the DESY laboratory and to the DESY accelerator group for their strong support since the conception of the HERA-B experiment. The HERA-B experiment would not have been possible without the enormous effort and commitment of our technical and administrative staff. It is not possible to list here the many individuals who have contributed to HERA-B. In the preparation of this paper, we have benefited from many useful discussions with A. Leibovich and J. Lee on the theory of heavy quarkonium production.

References

[1] R. Baier, R. Rückl, Phys. Lett. **B102** (1981)364; Z. Phys. **C19** (1983) 251

[2] G.T. Bodwin, E. Braaten, G.P. Lepage, Phys. Rev. **D51** (1995) 1125

[3] P. Cho, A. Leibovich, Phys. Rev. **D53** (1996) 6203

[4] H. Fritzsch, Phys. Lett. **B67** (1977) 217; F. Halzen, Phys. Lett. **B69** (1977) 105; F. Halzen, S. Matsuda, Phys. Rev. **D17** (1978) 1344; M. Glück, J. Owens, E. Reya, Phys. Rev. **D17** (1978) 2324 R. Gavai *et al.*, Int. J. Mod. Phys. **A10** (1995) 3043

[5] J. F. Amundson *et al.*, Phys. Lett. **B372** (1996) 127; Phys. Lett. **B390** (1997) 323

[6] C. Caso *et al.*, Review of Particle Physics, Eur. Phys. Jour. **C15** (2000) 1

[7] **E771** collab., T. Alexopoulos *et al.*, Phys. Lett. **B374** (1996) 271

[8] **ISR** collab., A.G. Clark *et al.*, Nucl. Phys. **B142** (1978) 29; **E610** collab., D.A. Bauer *et al.*, Phys. Rev. Lett. **54** (1985) 753; **E705** collab., L. Antoniazzi *et al.*, Phys. Rev. Lett. **70** (1993) 383; **E771** collab., T. Alexopoulos *et al.*, Phys. Rev. **D62** (2000) 032006

[9] **IHEP140** collab., F. Binon *et al.*, Nucl. Phys. **B239** (1984) 311; **WA11** collab., Y. Lemoigne *et al.*, Phys. Lett. **B113** (1982) 509; **E610** collab., D.A. Bauer *et al.*, Phys. Rev. Lett. **54** (1985) 753; **E673** collab., T.B.W. Kirk *et al.*, Phys. Rev. Lett. **42** (1979) 619; **E369** collab., S.R. Hahn *et al.*, Phys Rev. **D30** (1984) 671; **E705** collab., L. Antoniazzi *et al.*, Phys. Rev. Lett. **70** (1993) 383; **E672/E706** collab., V. Koreshev *et al.*, Phys. Rev. Lett **77** (1996) 4294

[10] **Belle** collab., K. Abe *et al.*, Phys. Rev. Lett. **88** (2002) 052001; **NA14** collab., R. Barate *et al.*, Z. Phys. **C33** (1987) 505

[11] G. Avoni *et al.*, Proc. of the IX Conference on Calorimetry in Particle Physics, Annecy, France, Oct. 9-14, 2000, Calorimetry in High energy physics (2001) 777

[12] **HERA-*B*** collab., E. Hartouni *et al.*, HERA-B Design Report, DESY-PRC-95-01 (1995); **HERA-*B*** collab., HERA-B Status Report, DESY-PRC-00-04 (2000)

[13] C. Bauer *et al.*, Nucl. Instr. Methods **A453** (2000)103

[14] **HERA-*B*** collab., I.Abt *et al.*, "Measurement of the $b\bar{b}$ Production Cross Section in 920 GeV Fixed-Target Proton-Nucleus Collisions", to be published in Eur. Phys. Jour. **C**; hep-ex/0205106

[15] T. Sjöstrand, Comp. Phys. Comm. **82** (1994) 74

[16] H. Pi, Comp. Phys. Comm. **71** (1992) 173

[17] R. Brun *et al.*, GEANT3, CERN-DD-EE-84-1 (1987)

[18] **CDF** collab., F. Abe *et al.*, Phys. Rev. Lett. **79** (1997) 578

[19] R. Vogt, Nucl. Phys. **A700** (2002) 539